Supplement: Exploring the climate system response to a range of freshwater representations: Hosing, Regional, and Freshwater Fingerprints

Ryan Love[1], Lev Tarasov[2], Heather Andres[3], Alan Condron[4], Xu Zhang[5], and Gerrit Lohmann[6,7]

[1]Department of Earth Sciences, University of Ottawa, Ottawa, Ontario, Canada
[2]Department of Physics and Physical Oceanography, Memorial University of Newfoundland, St. John's, Newfoundland, Canada
[3]Physical Scientist, Oceanography, Northwest Atlantic Fisheries Centre, Fisheries and Oceans Canada
[4]Geology & Geophysics, Woods Hole Oceanographic Institution, Woods Hole, Massachusetts, USA
[5]State Key Laboratory of Tibetan Plateau Earth System, Resources and Environment (TPESRE), Chinese Academy of Sciences (CAS), Beijing 100101, China
[6]Alfred Wegener Institute, Helmholtz Centre for Polar and Marine Research, Bremerhaven, Germany
[7]Department of Environmental Physics & MARUM, University of Bremen, Bremen, Germany

September 28, 2023

S1 Supplemental Figures

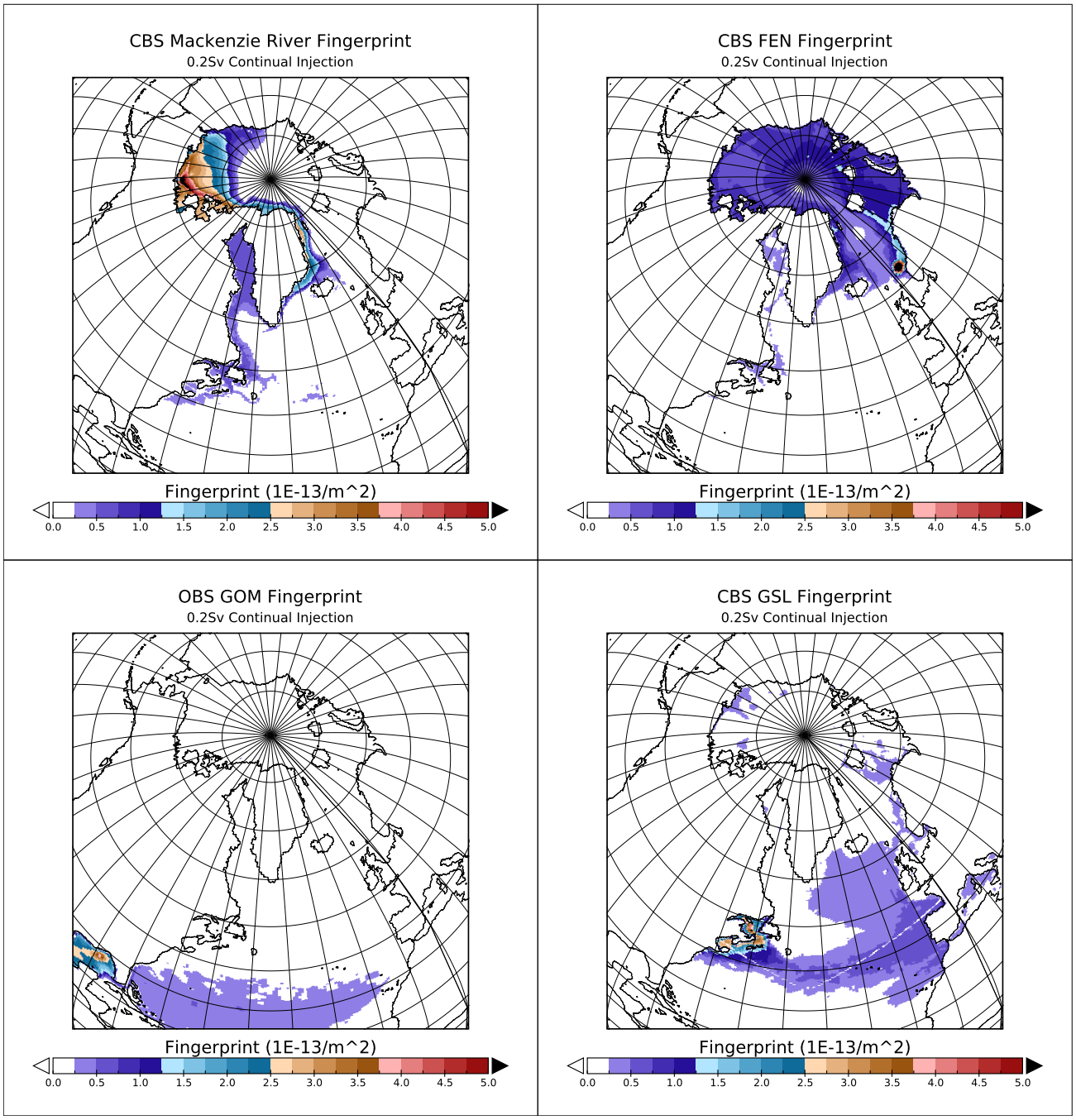

Figure S1: Each of the freshwater fingerprints used in this study. Values shown are the normalized values as on a regular $\frac{1}{6}^{\circ}$ global grid. To obtain an injection rate in $\frac{m}{s}$ for a given fingerprint simply multiply the shown distribution by the desired volume flux.

Figure S2: Freshwater injection locations for the generation of the fingerprints and regional injection locations. MAK is Mackenzie River, FEN is Fennoscandia, GSL is Gulf of St. Lawrence, GOM is Gulf of Mexico. Cape Hatteras and the Cabot Strait are shown with blue and purple circles respectively. Present day land-sea mask is shown in grey, Younger Dryas land-sea mask as used in Love et al. [2021] and the generation of the fingerprints is contoured in black, and the 38ka land-sea mask used in COSMOS is contoured in red. The 50-70N injection region is shown in yellow. The Barents-Kara sea region over which our freshwater flux calculation is done is shown in Green.

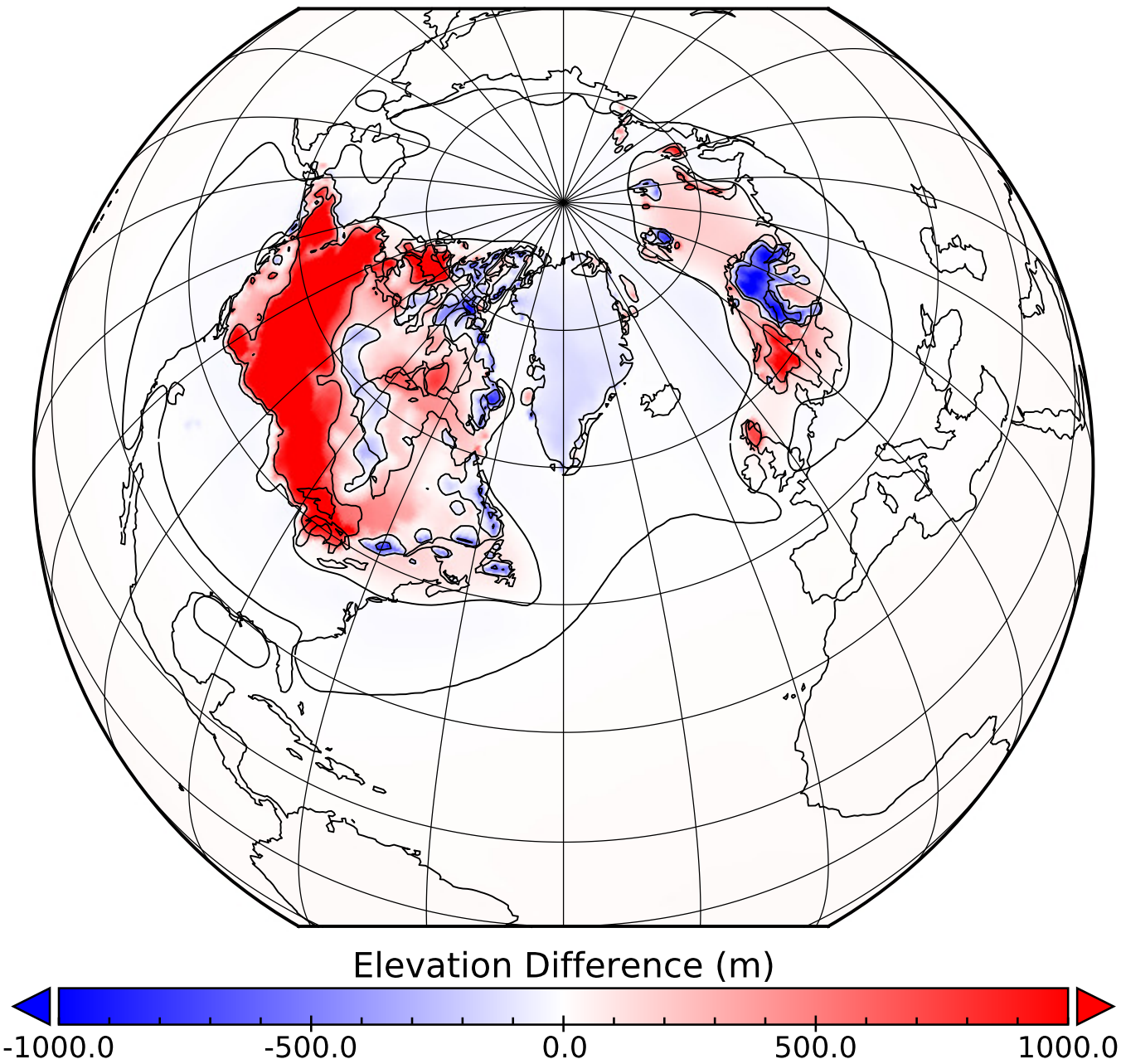

Figure S3: Difference in elevation at 38ka and 13ka from our reconstruction. Ice extent is largely the same except over western Canada where the North American Ice Complex is more extensive at 38ka. Sea level over the North Atlantic and Arctic is generally less than 10m difference while far field locations are $\approx$ 15m.

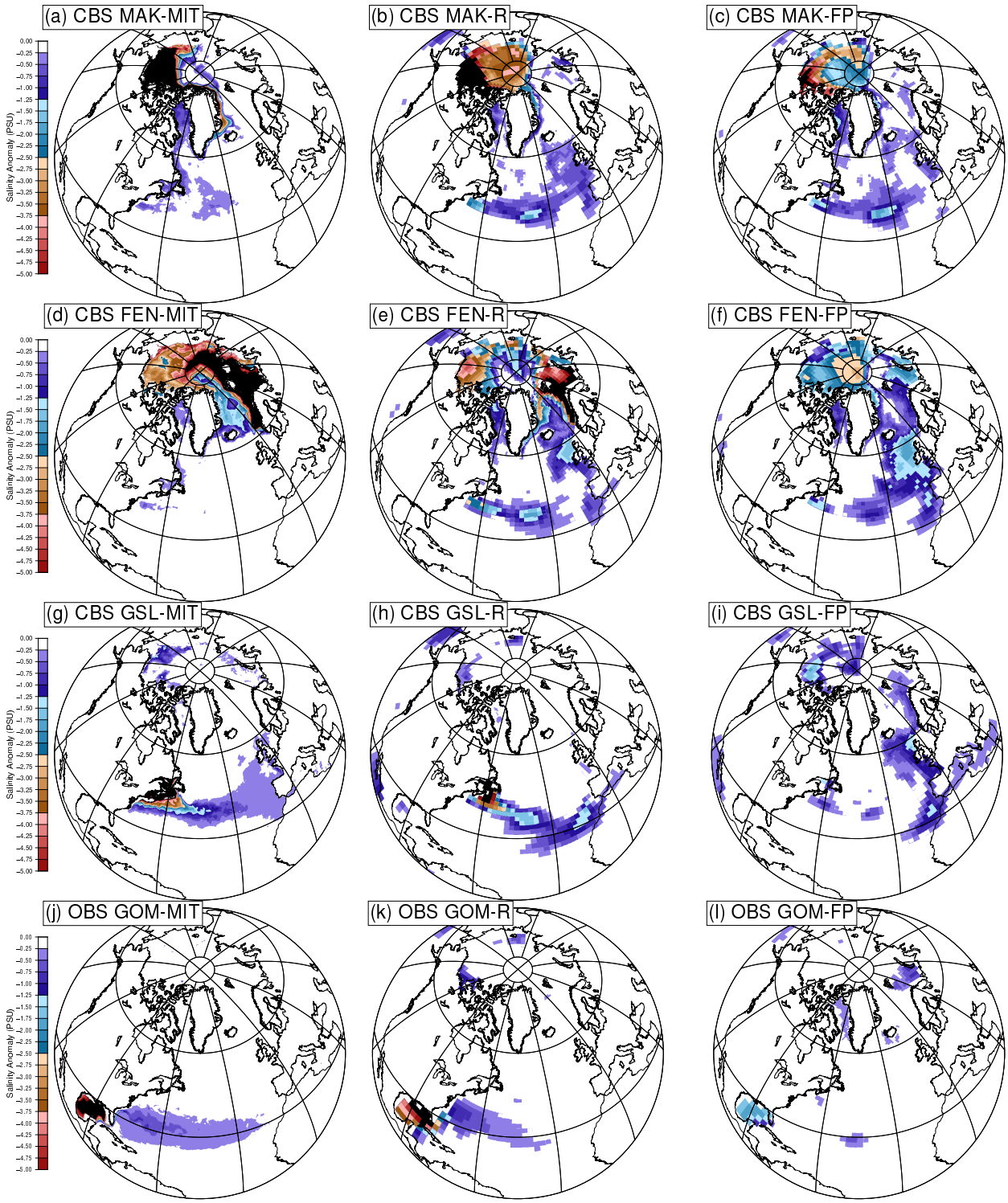

Figure S4: Salinity anomalies over the upper 30 m of the water column for the MITgcm (a/d/g/j) and the COSMOS-R (b/e/h/k), and COSMOS-FP(c/f/i/l) simulations for each of the outlets.

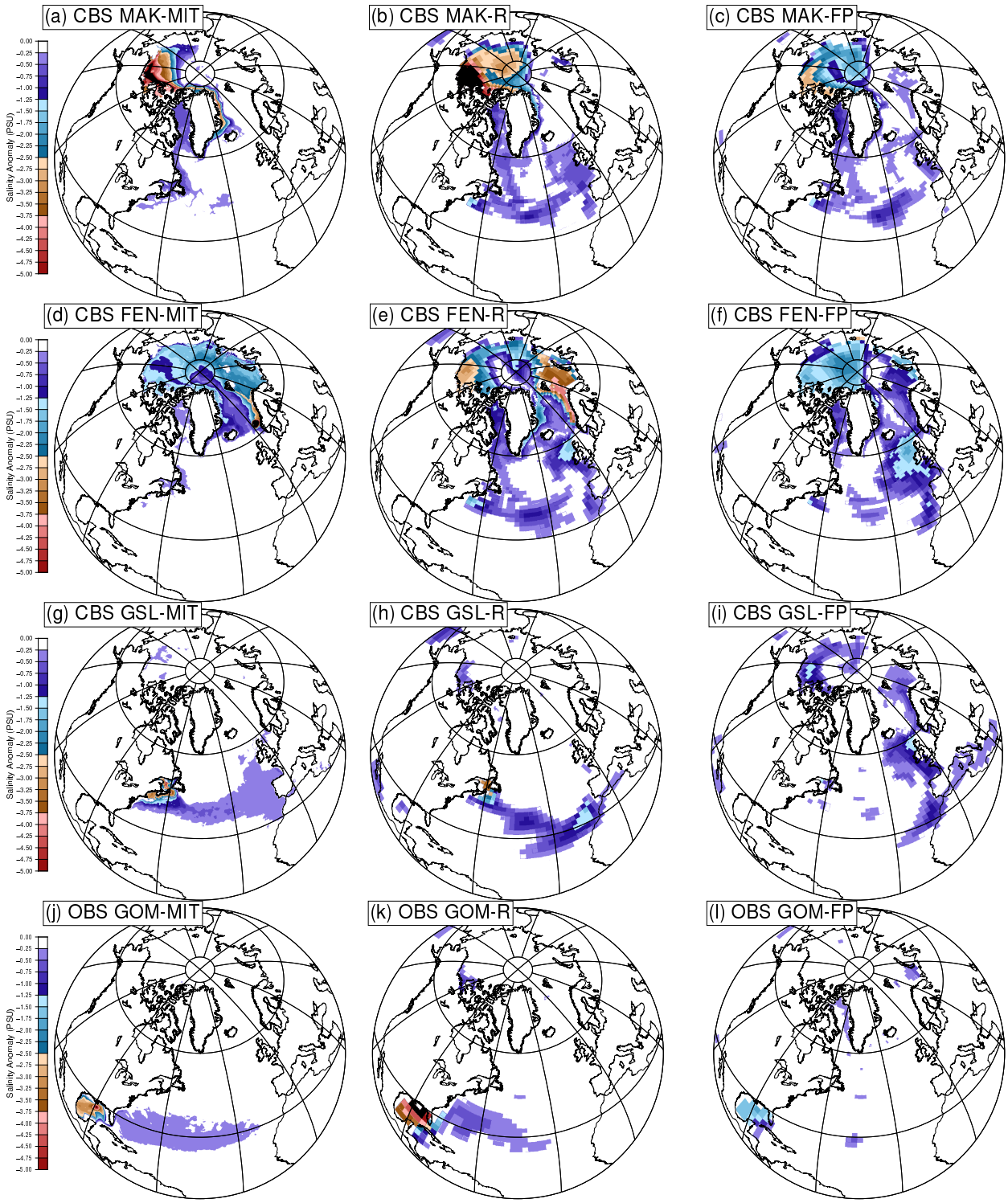

Figure S5: Salinity anomalies over the upper ≈ 100 m of the water column for the MITgcm (a/d/g/j) and the COSMOS-R (b/e/h/k), and COSMOS-FP(c/f/i/l) simulations for each of the outlets.

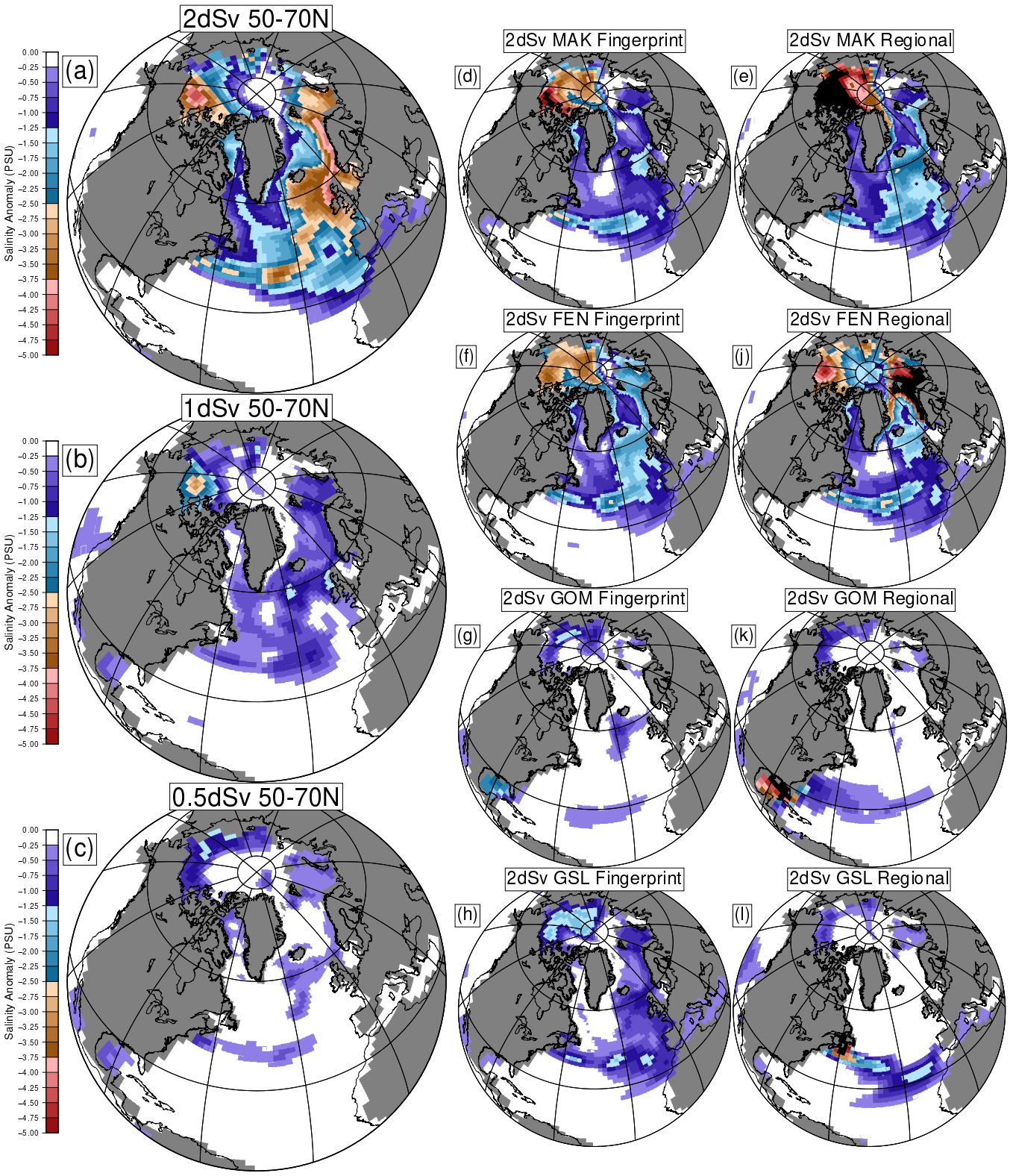

Figure S6: Salinity anomaly averaged over years $20-30$ of injection averaged over the top 30m of the water column. Subfigures a,b,c show the impact of a 50-70N injection with varying fluxes uniformly distributed over the band. Subfigures d,f,g,h, show the salinity anomalies resulting from using the fingerprint distributions with a 2dSv flux. Similarly, subfigures e,j,k,l show the salinity anomalies resulting from the regional injection locations.

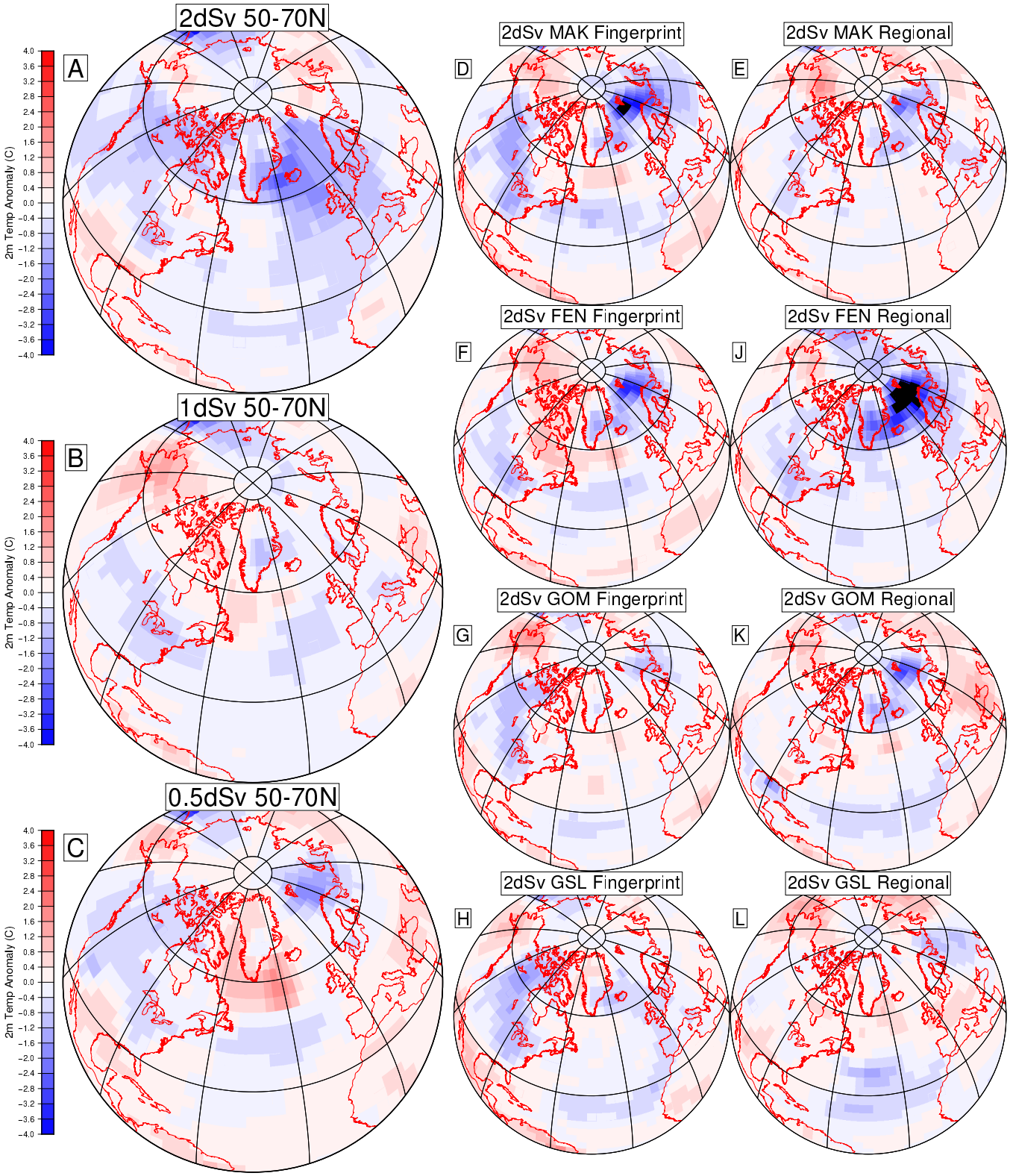

Figure S7: 2m temperature anomaly averaged over the first 10yr of injection. Subfigures a,b,c show the impact of a 50-70N injection with varying fluxes uniformly distributed over the band. Subfigures d,f,g,h, show the salinity anomalies resulting from using the fingerprint distributions with a 2dSv flux. Similarly, subfigures e,j,k,l show the salinity anomalies resulting from the regional injection locations.

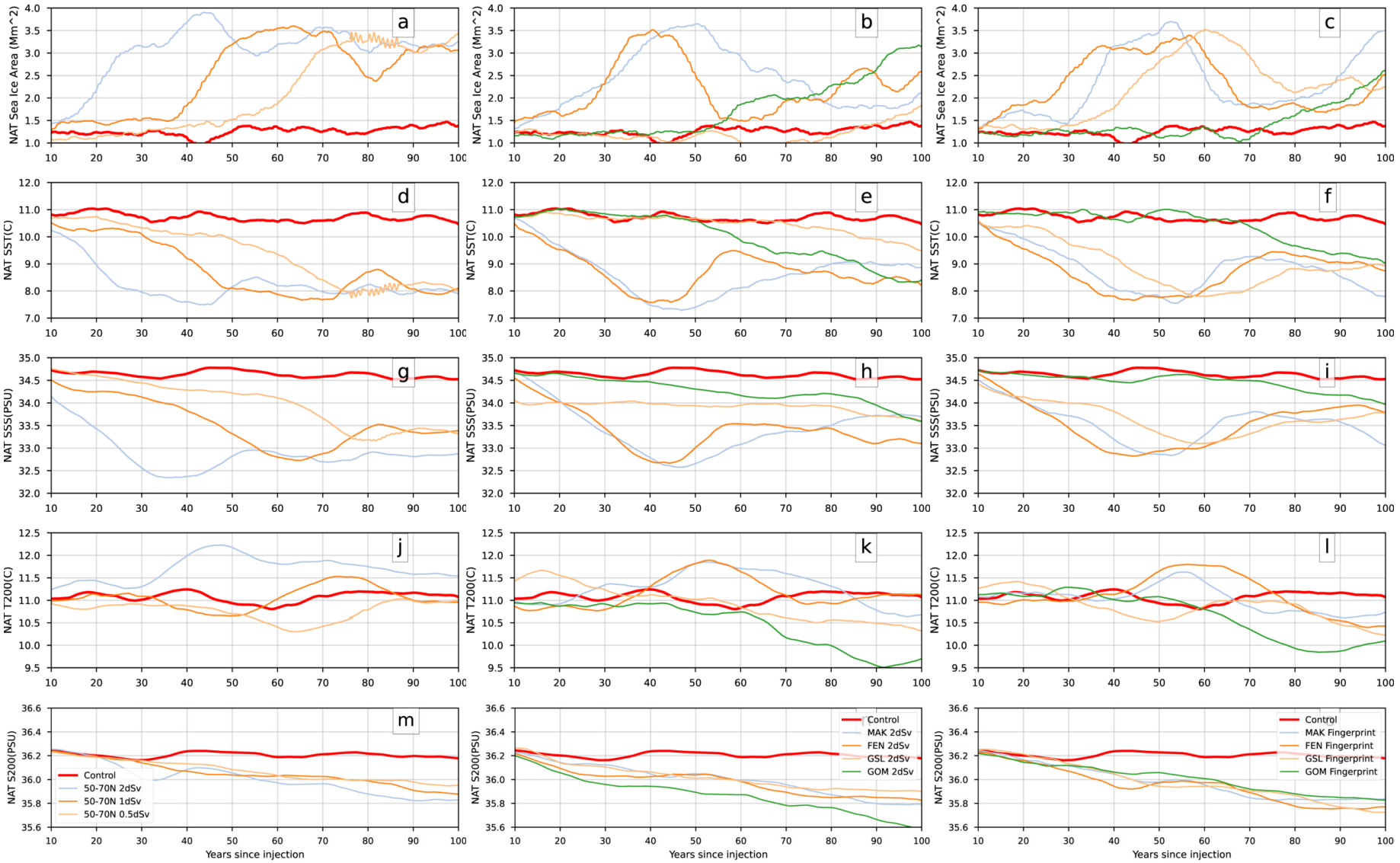

Figure S8: Ocean domain metrics for the upper layers of the North Atlantic Ocean. Each of the timeseries shown are boxcar running mean with a 10 year window.

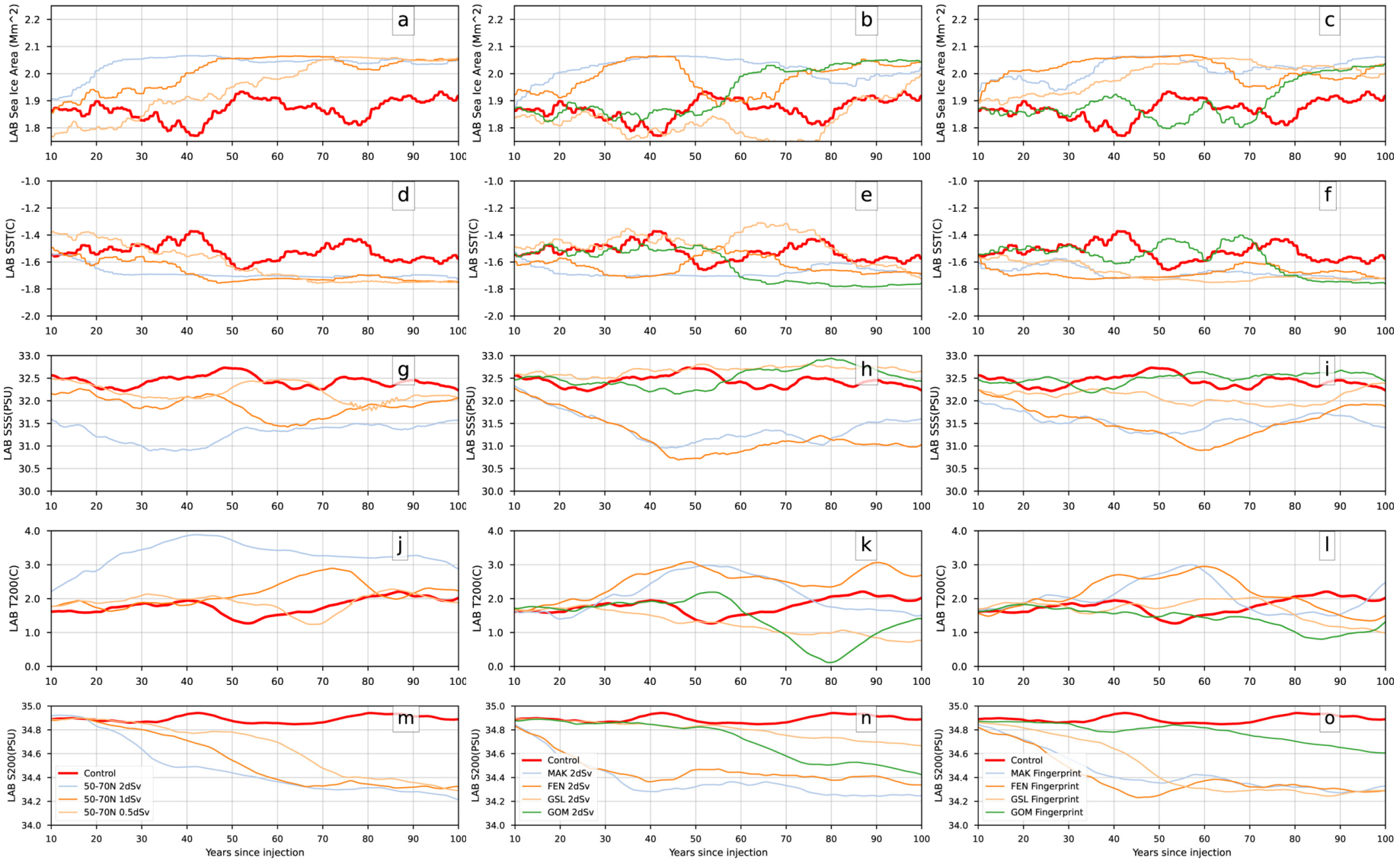

Figure S9: Ocean domain metrics for the upper layers of the Labrador Sea. Each of the timeseries shown are boxcar running mean with a 10 year window.

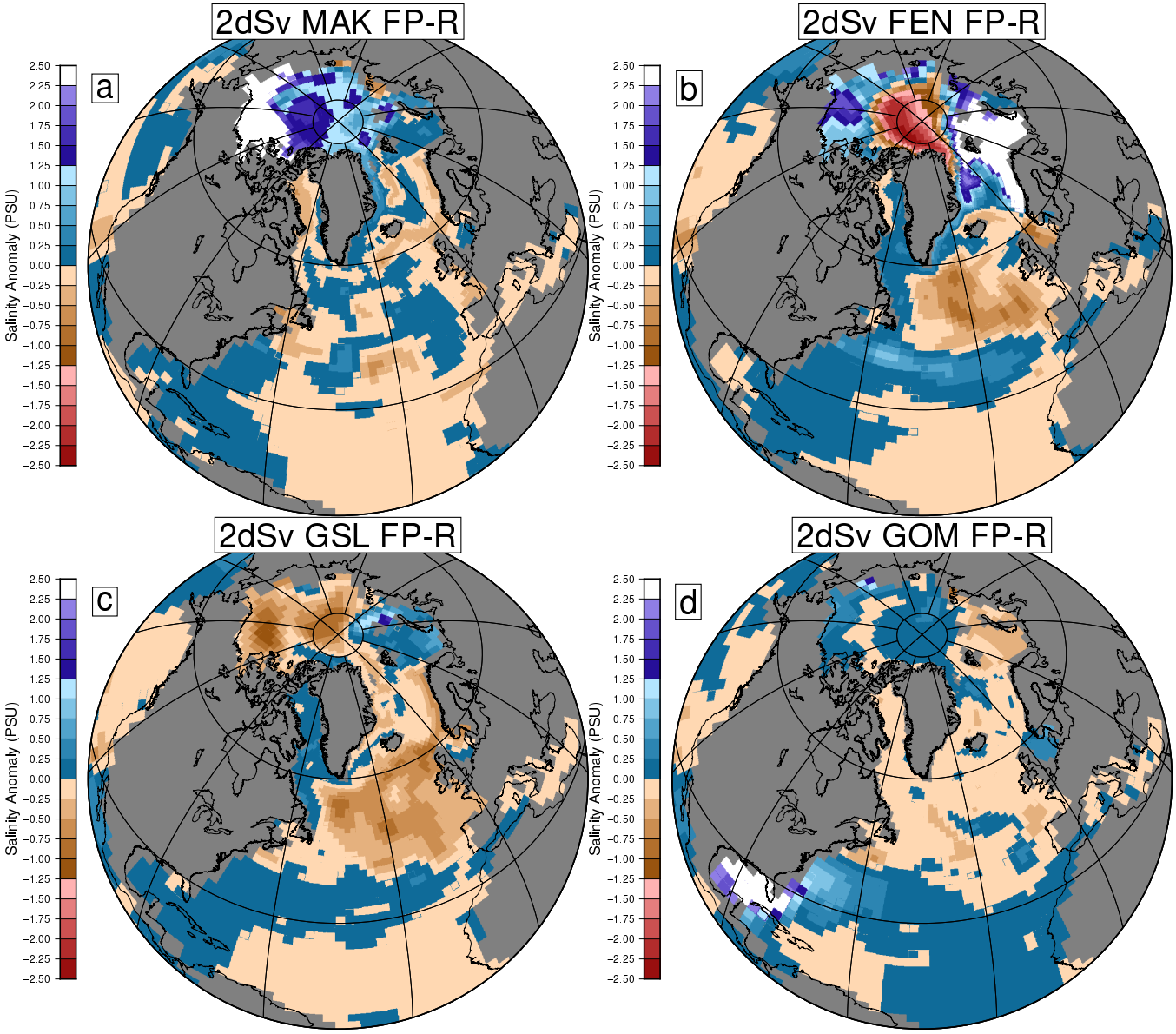

Figure S10: Difference in the salinity fields between the fingerprint and regional injection methods used in COSMOS for each outlet. The salinity field shown is averaged over years $10-20$ of injection averaged over the top 30m of the water column. Positive values correspond to regions where the regional injection results in greater freshening, while negative values correspond to regions where the fingerprint injection results in greater freshening, relative to each other.

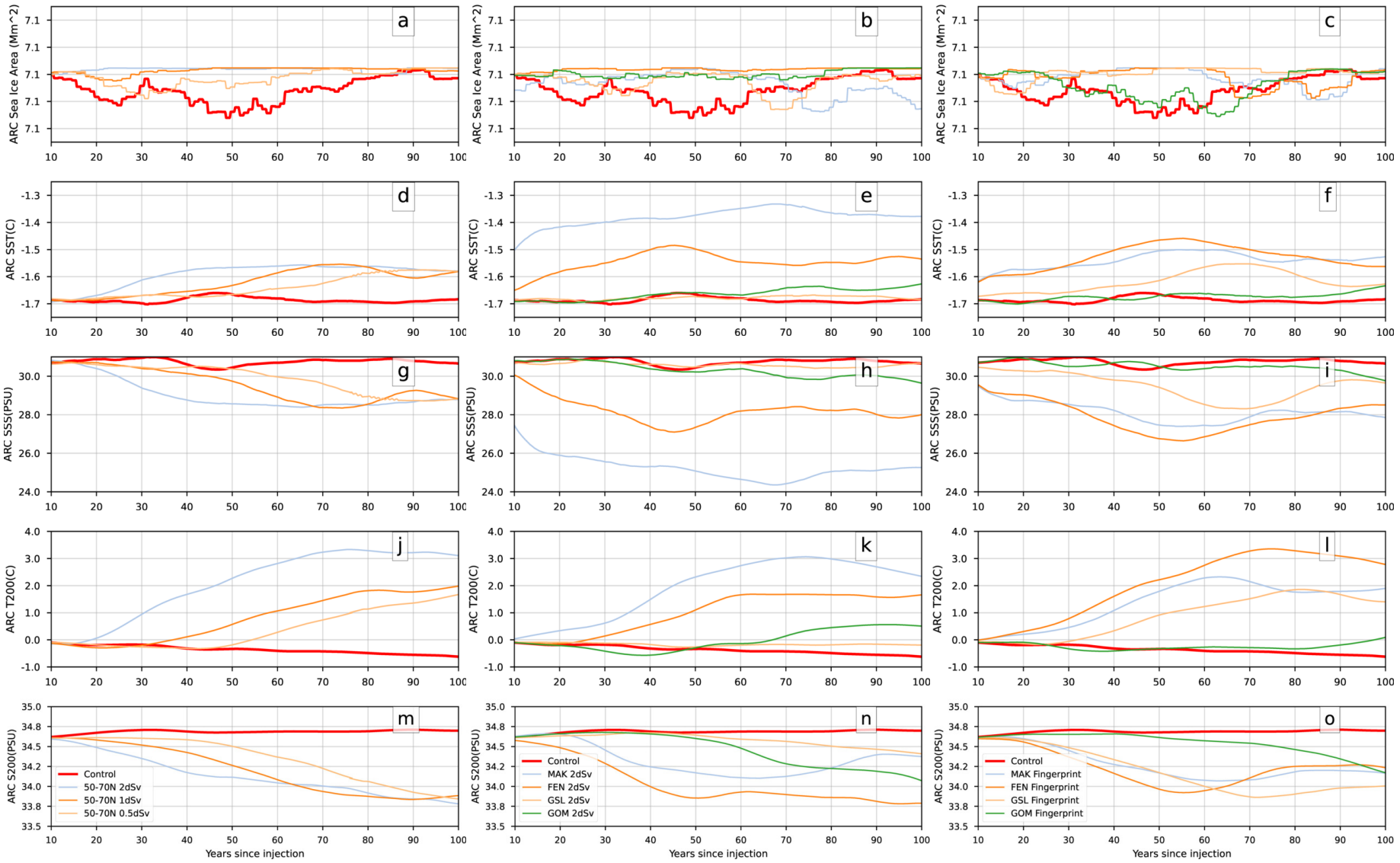

Figure S11: Ocean domain metrics for the upper layers of the Arctic Ocean. Each of the timeseries shown are boxcar running mean with a 10 year window.

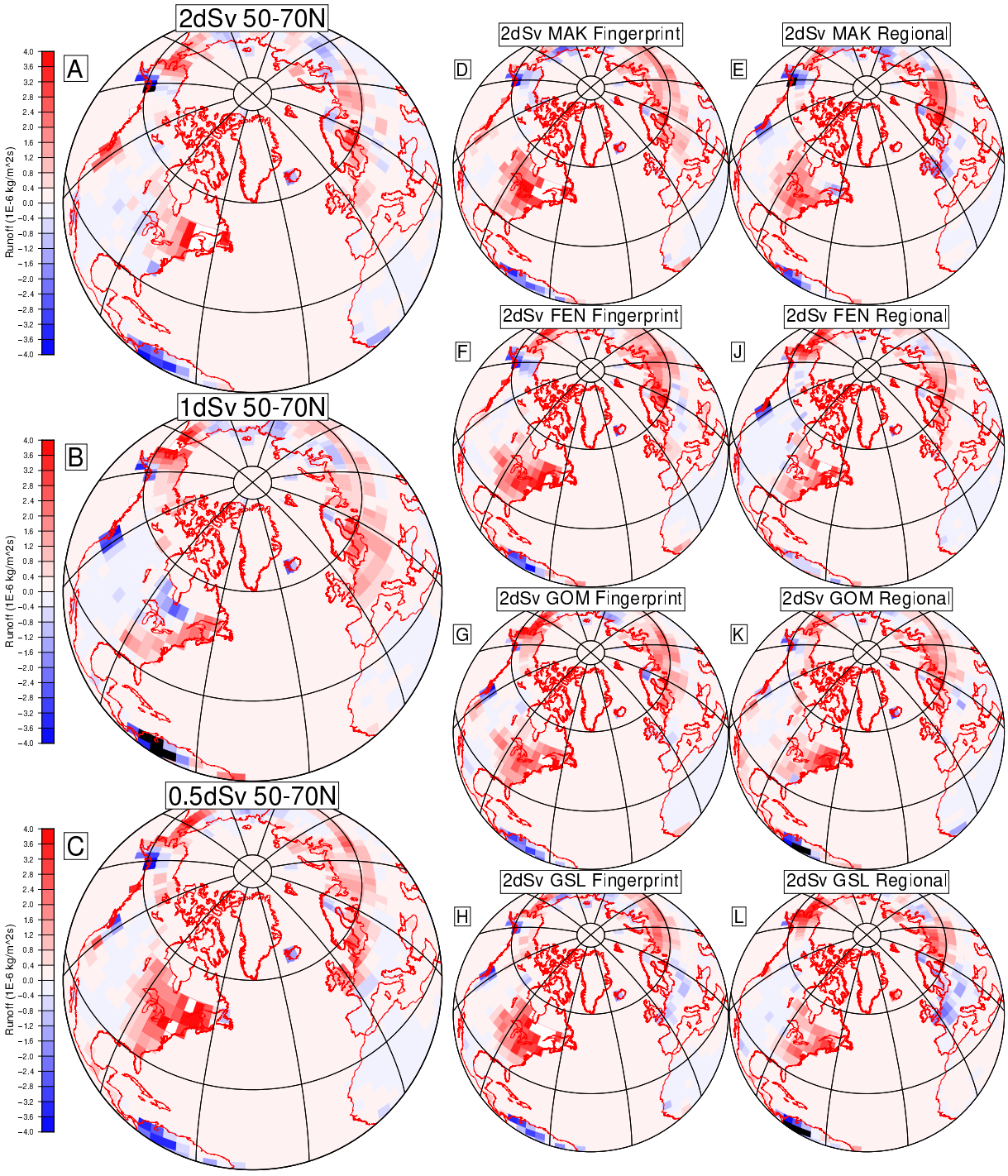

Figure S12: Surface runoff anomaly averaged over the first 10yr of injection. Subfigures a,b,c show the impact of a 50-70N injection with varying fluxes uniformly distributed over the band. Subfigures d,f,g,h, show the salinity anomalies resulting from using the fingerprint distributions with a 2dSv flux. Similarly, subfigures e,j,k,l show the salinity anomalies resulting from the regional injection locations.

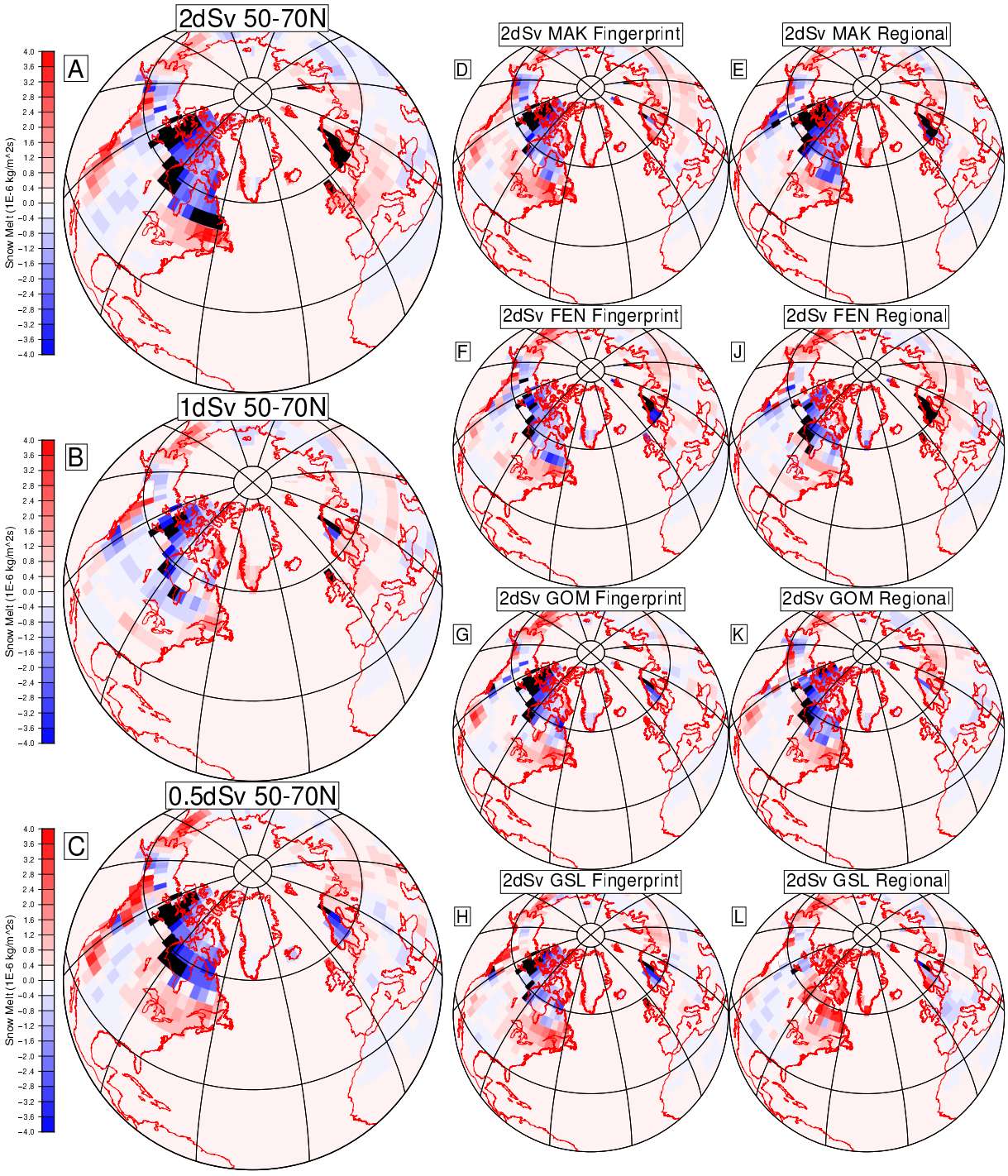

Figure S13: Snow melt anomaly averaged over the first 10yr of injection. Subfigures a,b,c show the impact of a 50-70N injection with varying fluxes uniformly distributed over the band. Subfigures d,f,g,h, show the salinity anomalies resulting from using the fingerprint distributions with a 2dSv flux. Similarly, subfigures e,j,k,l show the salinity anomalies resulting from the regional injection locations.

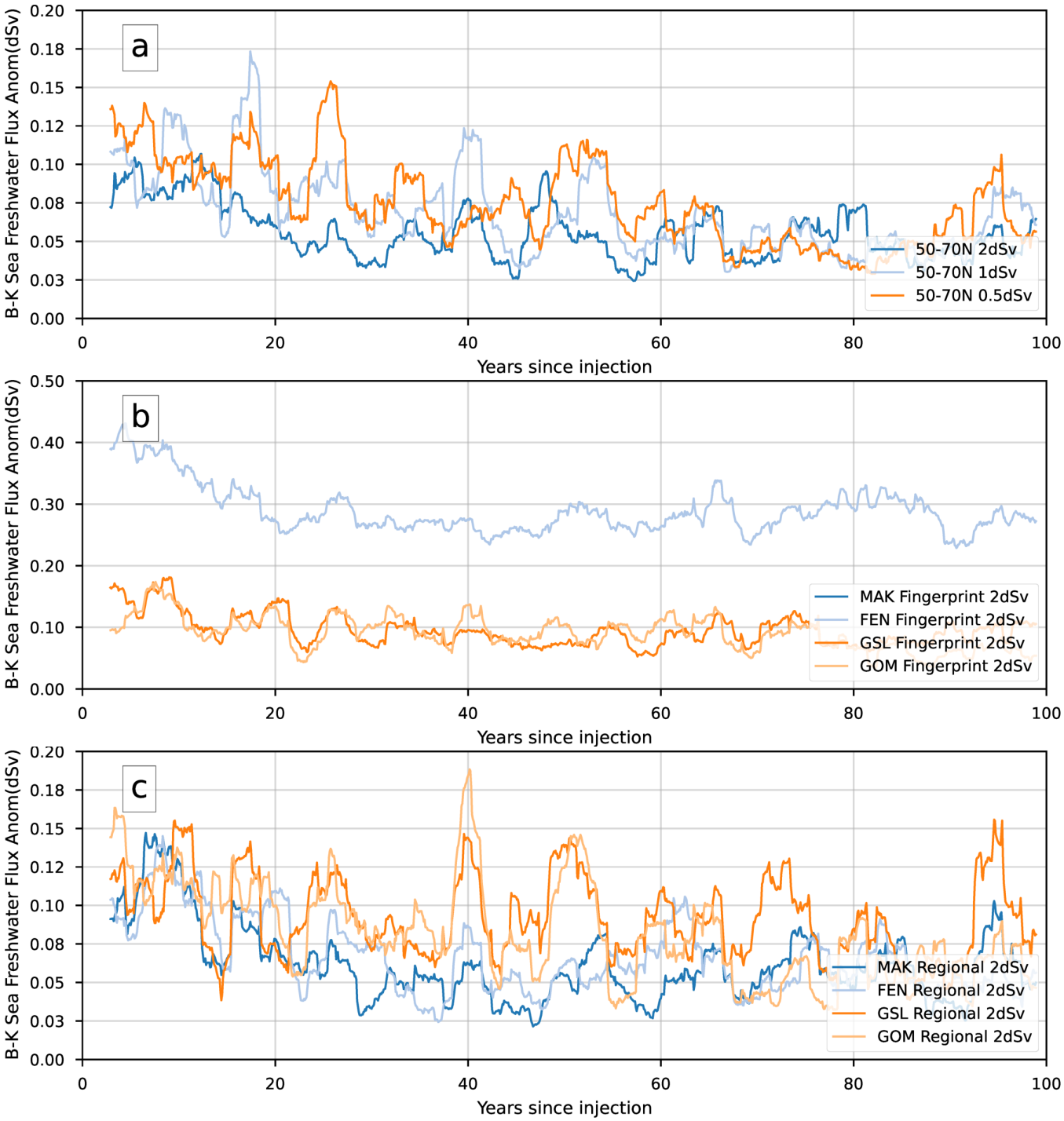

Figure S14: Freshwater flux into the Barents-Kara Sea, the green region in fig. S2. In sub-figure b the Fennoscandia fingerprint run is off the scale due to the fingerprint injection itself overlapping with the region. We note that it does not show the rise in variability as in the other timeseries shown. Similarly, the large value for the Mackenzie River fingerprint also has some overlap with the region.

S2 Overly zonal winds in MITgcm and resulting impacts

Love et al. [2021] showed that this feature results in freshwater introduced south of the Gulf Stream being transported more southward relative to a less zonal configuration (when considering the latitude at which freshwater impinges on eastern border of the Atlantic). It is also shown that when using less zonal winds (in the ERA40 simulations of Love et al. [2021]) that the freshwater was deposited slightly closer to sites of deep water formation as the Gulf Stream was more north-easterly than with LGM winds. In this study, the impact of wind forcing is most relevant for the Gulf of Mexico and Gulf of St. Lawrence fingerprints. Glacial runoff from these outlets is mostly entrained by the Gulf Stream, but this entrainment more strongly affects the GOM as the Gulf Stream acts as a northern limit to freshwater transport, separating freshwater from the sites of deep water formation no matter the orientation. Our fingerprint resultantly deposits freshwater further south of sites of deep water formation relative to a fingerprint generated from a simulation where the Gulf Stream is more tilted like at present.

S3 COSMOS Derived Fingerprint Comparison

In comparing the COSMOS-derived fingerprint fields to the MITgcm fingerprints, Figs. 2 and 1 respectively, we find large-scale differences in the distributions that are not as readily visible when comparing the salinity distributions. Here again, the slower rate of freshwater transport is readily demonstrated, as all COSMOS regional injection experiments show much less freshwater downstream of the injection locations. The fingerprint marginal gradients in the eddy-permitting configuration are also generally sharper when compared to the coarse resolution configuration, readily demonstrating the strongly diffusive nature of the coarser resolution configuration. A significant proportion of MAK-R freshwater extends into the central Arctic (loosely following Lomonosov Ridge) relative to the MAK-MIT fingerprint, such that MAK-MIT has both a larger concentration of freshwater at the mouth of the Mackenzie and a greater transport of freshwater downstream into the North Atlantic than MAK-R for the same amount of injection. FEN-R shows minimal freshwater coverage over the interior of the GIN Seas or central Arctic relative to the FEN-MIT fingerprint, with much of the freshening occurring downstream in the Barents-Kara Seas and Beaufort Sea. Of note is a secondary salinity minimum at the mouth of the Mackenzie in FEN-R that is not present in FEN-MIT. This feature is discussed in more detail in Supplemental Section S4. GSL-R shows a markedly different distribution relative to the GSL-MIT fingerprint. The GSL-MIT fingerprint features southward advection along the North American coast toward Cape Hatteras, followed by a largely zonal band of freshening, which aligns with the Gulf Stream. Upon reaching the coast of Europe, the freshwater is mixed both northward and southward along the coast, with the majority of the freshwater heading north. Comparatively, the GSL-R fingerprint shows freshwater is transported directly south-east across the Gulf Stream and becomes entrained in the sub-Tropical gyre. GOM-R is the most similar to its respective fingerprint, but this is largely a result of freshwater entrapment within the Gulf of Mexico dominating the signal. Downstream from the injection location, fingerprint values, and thus salinity anomalies, are generally smaller than in the MITgcm fingerprint. Given these results, it appears the slower rate of tracer transport in the eddy parameterizing model counterbalances the lack of Caribbean Islands constricting flow out of the Gulf of Mexico.

S4 Why do we have such a strong salinity anomaly in Barents-Kara?

A feature common to all our injection scenarios is a strong salinity anomaly in the Barents Kara sea. Examination of the runoff field shows that all simulations show enhanced surface runoff into this region, see fig S12. This runoff is explained by enhanced surface warming and snow-melt over North Asia and Eastern Europe, see figs S7 and S13 respectively. This enhanced runoff into the Barents-Kara sea, and to a lesser extent the GIN seas, serves to amplify the climate response of a given flux of freshwater by $\approx 4 - 10\%$ of the total freshwater signal. Figure S14 shows that the peak of the enhanced runoff is short-lived but an enhanced runoff signal is present in all injection scenarios. This feature is similarly replicated around the Mackenzie River for our FEN-R simulation.

S5 Impact of Open Bering Strait Fingerprints

Open Bering Strait (OBS) fingerprints were generated and evaluated for the Fennoscandian (FEN) and Gulf of St. Lawrence (GSL) injection scenarios (as described in Table S1) These fingerprints and resultant COSMOS simulations are in addition to the closed Bering Strait (CBS) fingerprints presented in the main paper. We note that while the fingerprints use the OBS configuration of the MITgcm, the COSMOS simulations still feature a CBS. The use of these fingerprints do not affect the conclusions of the main text. Select figures comparable to those for the CBS configurations of the FEN and GSL fingerprints are shown here for interest and comparison. We note that the use of an OBS GOM was a result of experimental design choices inherited from Love et al. [2021]. However, given the results of this investigation we anticipate no significant impact from this feature.

Run Short Name	Model	Continual Freshwater Forcing Distribution	Background Climate
FEN-MIT-OBS	MITgcm	2 dSv FEN Regional	OBS Hybrid LGM/YD
GSL-MIT-OBS	MITgcm	2 dSv GSL Regional	OBS Hybrid LGM/YD
FEN-FP-OBS	COSMOS	2 dSv FEN Fingerprint (FEN-MIT-OBS derived)	38ka Orbital and GHG
GSL-FP-OBS	COSMOS	2 dSv GSL Fingerprint (GSL-MIT-OBS derived)	38ka Orbital and GHG

Table S1: As in Table 1 but describing the two additional MITgcm simulations from which the OBS FEN and OBS GSL fingerprints are derived. The background hybrid LGM/YD climate is as follows: 13 ka Bathymetry, LGM Ocean Surface Forcing, and an open Bering Strait. The MITgcm simulations were conducted using the cs510 grid which is roughly $\frac{1}{6}^{\circ}$/18 km horizontal resolution with 50 vertical levels and are the same simulations as described in Love et al. [2021].

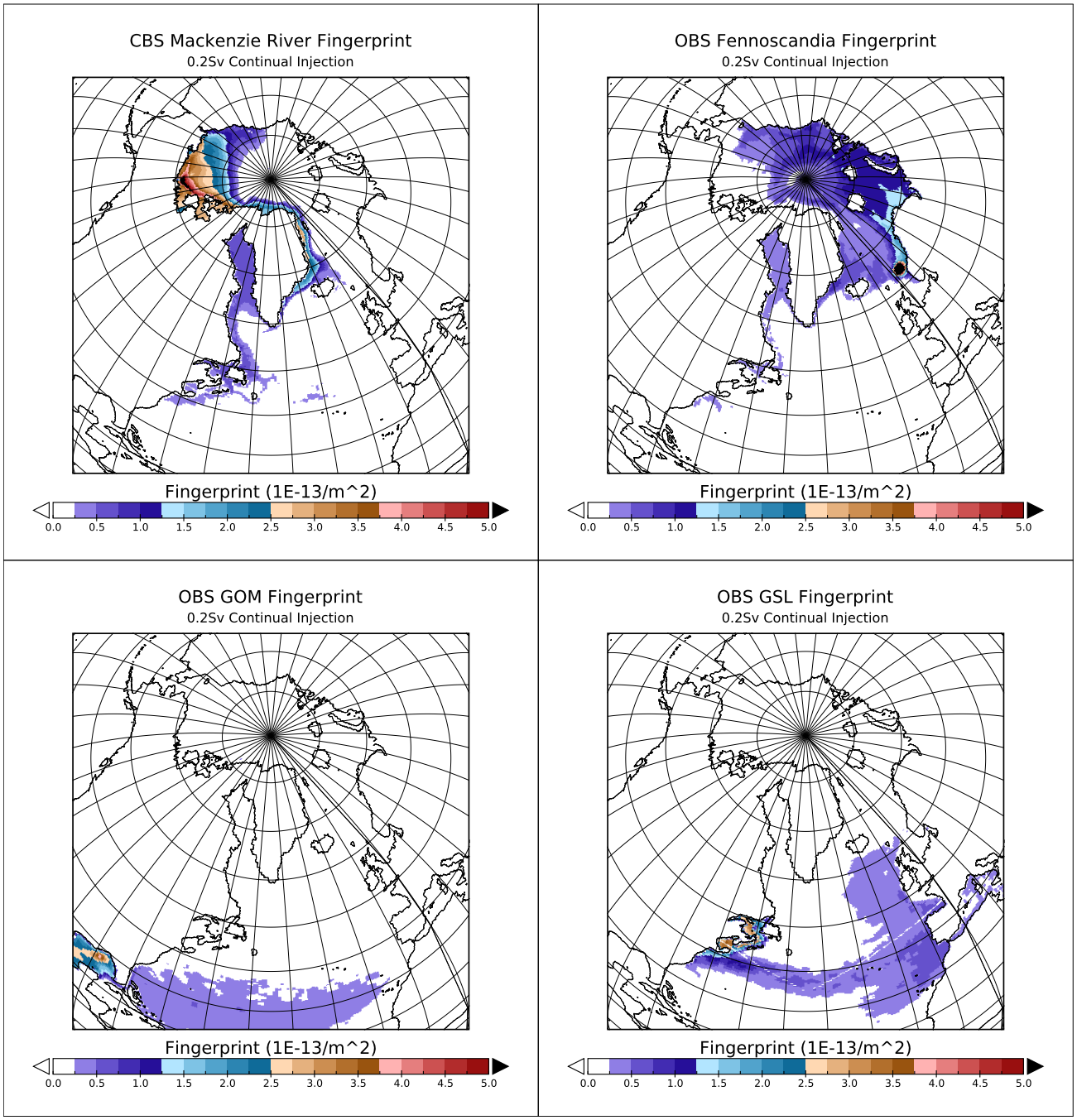

Figure S15: Each of the freshwater fingerprints used in this study as in Fig. S1 but with OBS GSL and FEN. Values shown are the normalized values as on a regular $\frac{1}{6}^{\circ}$ global grid. To obtain an injection rate in $\frac{m}{s}$ for a given fingerprint simply multiply the shown distribution by the desired volume flux.

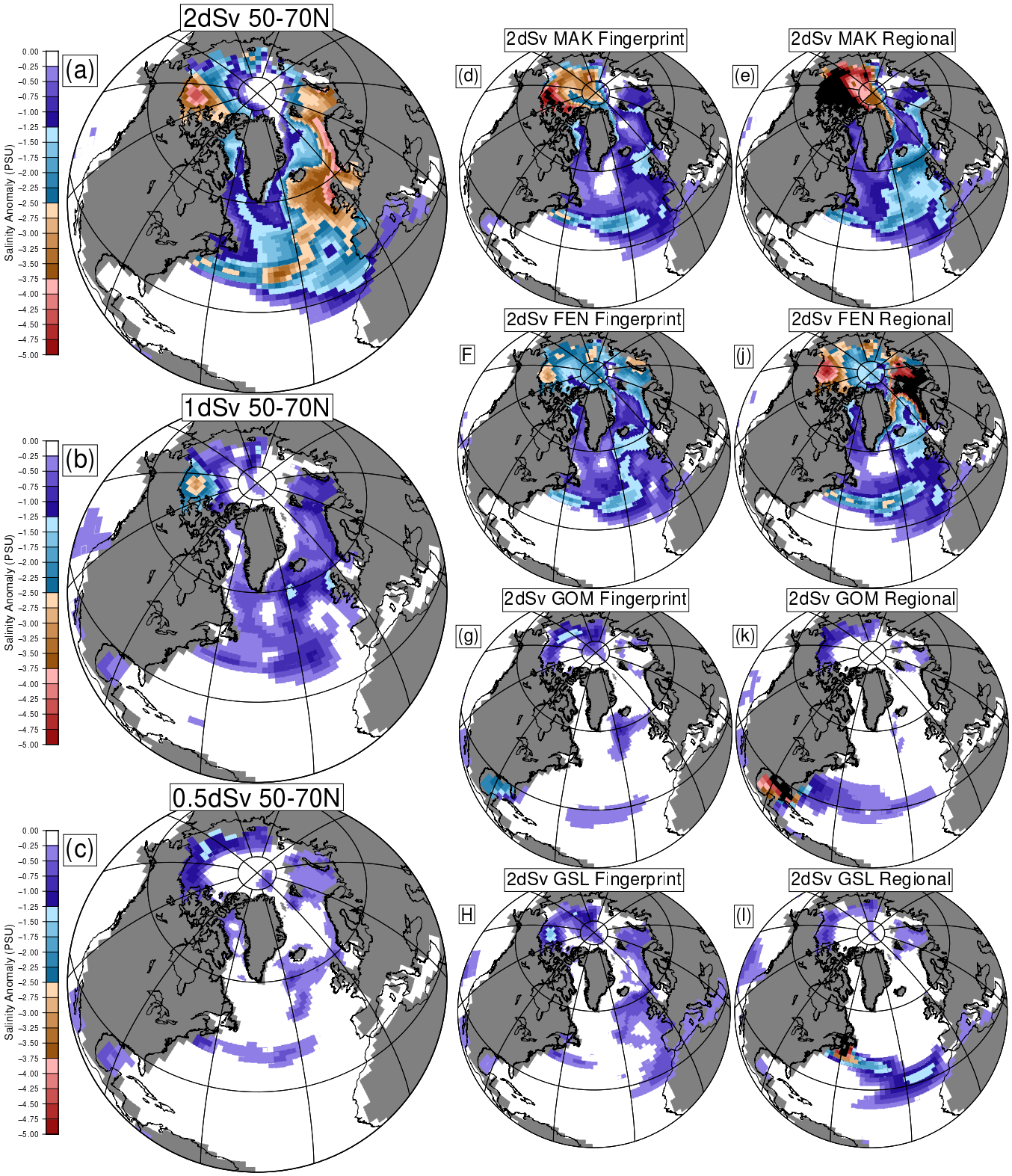

Figure S16: Same as Fig. S6 but using OBS FEN and GSL fingerprints in subfigures f and h respectively. Salinity anomaly averaged over years $20-30$ of injection averaged over the top 30m of the water column. Subfigures a,b,c show the impact of a 50-70N injection with varying fluxes uniformly distributed over the band. Subfigures d,f,g,h, show the salinity anomalies resulting from using the fingerprint distributions with a 2dSv flux. Similarly, subfigures e,j,k,l show the salinity anomalies resulting from the regional injection locations.

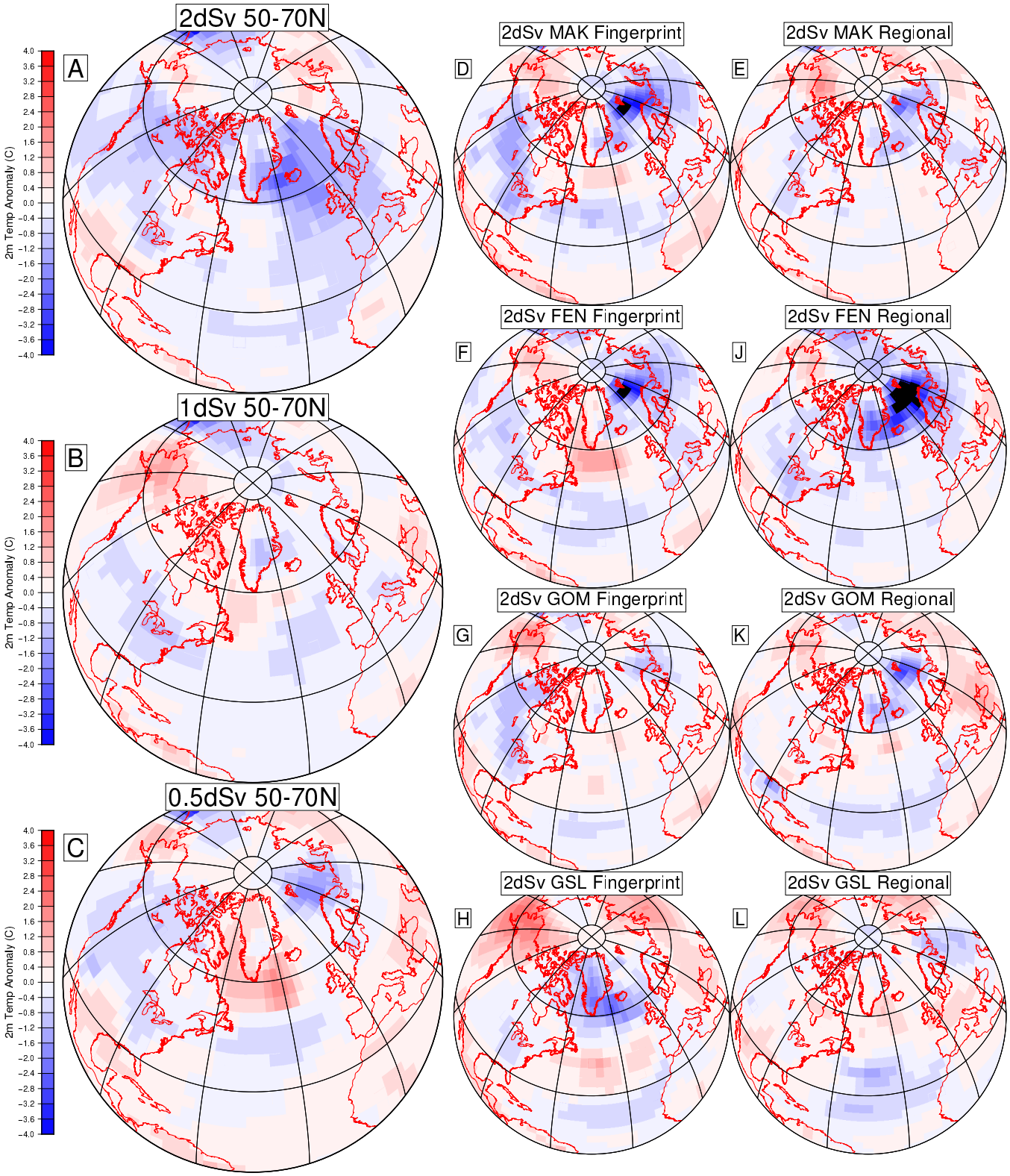

Figure S17: Same as Fig. S7 but using OBS FEN and GSL fingerprints in subfigures f and h respectively. 2m temperature anomaly averaged over the first 10yr of injection. Subfigures a,b,c show the impact of a 50-70N injection with varying fluxes uniformly distributed over the band. Subfigures d,f,g,h, show the salinity anomalies resulting from using the fingerprint distributions with a 2dSv flux. Similarly, subfigures e,j,k,l show the salinity anomalies resulting from the regional injection locations.

S6 Blending of MAK Fingerprint and Regional Injections

As discussed in the main text, one of the shortcomings of the fingerprint method is the discrepancy in the salinity anomaly distribution between the fingerprint injections and either of the regional injection methods. As shown in Figs. S4 and S5 the salinity anomalies resulting from use of the fingerprints are generally more different to the MITgcm simulations than the regional injections. This results from two aspects, the more diffuse nature of the fingerprint injections results in the freshwater being more readily mixed into the water column (due to the lower density contrasts vs. regional injection), and not accounting for the inherent transports in the model. To attempt to mitigate these shortcomings we evaluated four blends of the fingerprint and regional injection distributions for the MAK region. The MAK-R and MAK-FP injection distributions were blended such that the flux for each simulation, 2 dSv as in the main text, was the same. We explored 3 intermediate ratios, as well as an additional extreme ratio of 0.1 fingerprint to 0.9 regional injection. This extreme ratio was guided by a simple correction field for the fingerprint. The correction field, B, was constructed such that $FP_{\text{corrected}} = B * FP$. As such we use $B = (S_{\text{MIT}} - S_{\text{MIT-control}})/(S_{\text{FP}} - S_{\text{COSMOS-control}})$. Examination of this correction field, which indicates a strong increase in the weight of upstream injection and a strong decrease in downstream injection by roughly a factor of 10, lead us to include the more extreme ratio. The resulting salinity anomaly distributions for these simulations, over the same interval as shown in Fig. S4, are shown in Fig. S18. Comparing the mean-square-errors of the salinity fields of each of the blends, the regional, and the fingerprint injection simulations to the MIT-MAK simulation's salinity anomaly field we find no improvement from including the blend. In summary, neither the fingerprint or the fingerprint:regional injection blends result in a salinity anomaly distribution which is more like the MIT-MAK salinity anomaly distribution than the COSMOS-R simulation when compared using the time interval which is used to generate the fingerprints themselves.

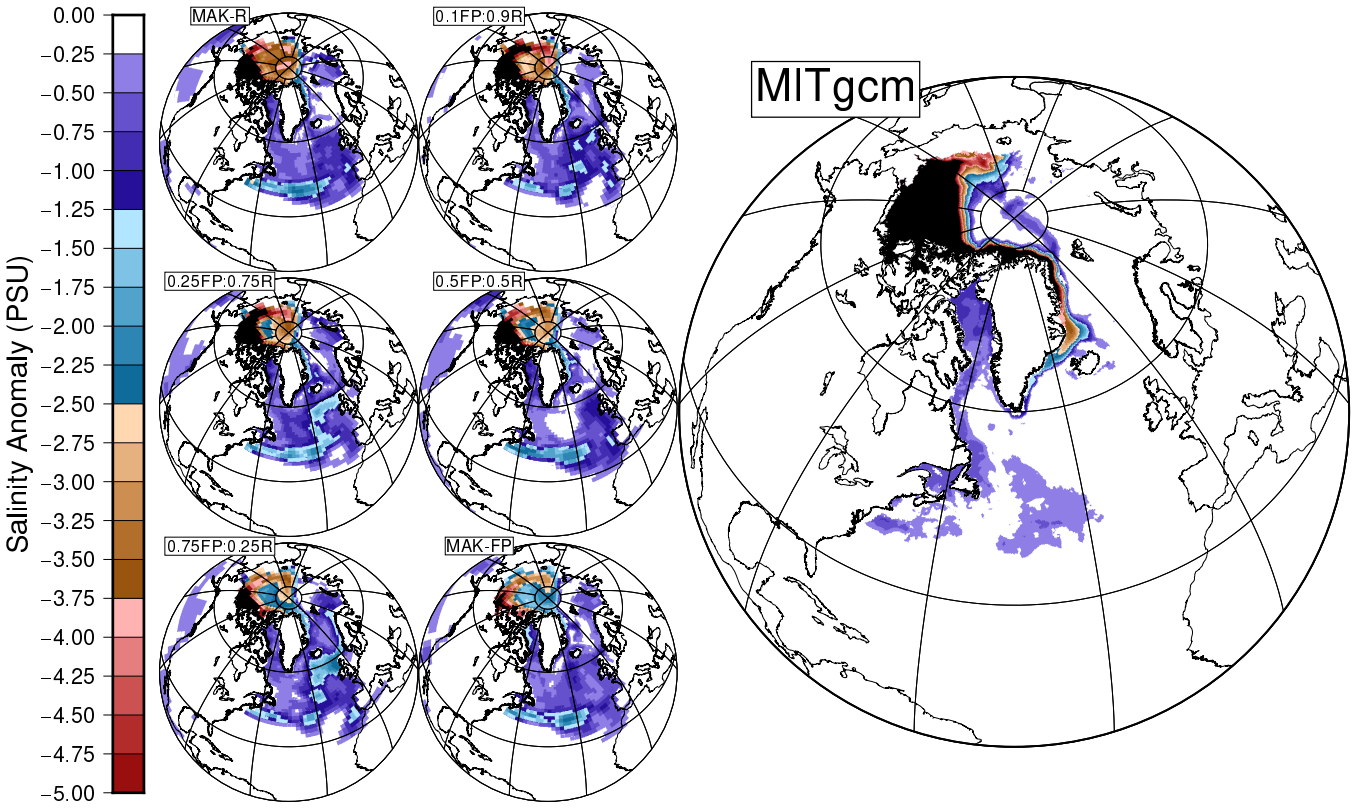

Figure S18: Salinity anomaly of top 30 m for various blends of the MAK-R and MAK-FP injection masks implemented in COSMOS. The salinity anomaly was averaged over the same time interval as for the MAK fingerprint generation. Far right-hand panel is the equivalent salinity anomaly from the MITgcm MAK-R simulation.

References

R. Love, H. Andres, A. Condron, and L. Tarasov. Eddy permitting simulations of freshwater injection from major northern hemisphere outlets during the last deglacial. *Climate of the Past Discussions*, 2021:1–16, 2021. doi: 10.5194/cp-2021-15. URL https://cp.copernicus.org/preprints/cp-2021-15/.